Small-Diameter Membrane Reflector Wrinkling

A. Bonin* and K. A. Seffen†
University of Cambridge, Cambridge, CB2 1PZ, UK
M. J. Santer‡
Imperial College London, London, SW7 2AZ, UK

This study concerns the wrinkling performance of thin membranes for use as novel reflectors in space-based telescopes. We introduce small-scale experiments for inducing and interrogating wrinkling patterns in flat membranes, and we capture these details computationally by performing a range of finite element analysis. The overall aim is to assess the sophistication of modelling, to verify the feasibility of a small-diameter reflector concept proposed in accompanying work.

I. Introduction

In our companion paper[1] we consider the merits of membrane reflectors for use as small-diameter, space-based telescopes in comparison to conventional monolithic reflectors. Specifically, we focus upon membrane reflectors with apertures similar in size to the Hubble Space Telescope, up to 3.5 m, which can fit into existing launch fairings without folding or being in disparate parts. It is shown that the areal density, the ratio of the area of reflector to its mass, can compete favourably with current technologies.

The lightness of membrane is key to this success, but it must be pre-tensioned for optical correctness, in order to eliminate anomalous surface distortions during operation. Tensile forces are applied to the membrane boundary that, in turn, are carried by a supporting edge structure. We propose a ring-truss for this structure[1] with a polygonal planform whose constituent bars only carry axial loads so that the overall mass performance is governed by the Euler buckling capacity and vibrational stiffness of bars. The membrane is subjected to discrete forces, which means that the membrane has the same polygonal form as the support structure. Specifically, the forces are carried at nodal junctions on the ring-truss via interconnecting cables to the membrane vertices. The number of polygon sides, denoted by n, is now an additional design variable and, ideally, this number is large, resulting in minimal cable forces for a given level of pre-strain and in a lighter edge structure. Practically, a large n adds complexity and extra mass for it is desirable to control each cable force in view of the refinement of the overall surface shape. Indeed, we have shown[1] that fewer gains in structural optimality alone are achieved when $n > 10$, and this is expected to be a reasonable upper limit for any realistic reflector.

However, the discrete features of the proposed concept can increase the possibility of membrane *wrinkling* in two ways, particularly for a low number of sides. First, the required cable forces for pre-tensioning generally increase as n decreases, which introduces higher tensile stresses at the vertices and, consequently, higher orthogonal compression. Second, should one of the cables fail, the degree to which shape control can be apportioned through the remaining intact cables is reduced, leading to asymmetrical membrane loads and a disruption of the desired biaxial stress state. Note that we assume that the membrane is initially flat, without any material wrinkles.

In our companion paper, the effects of membrane wrinkling are not dealt with explicitly as it may be reasonably assumed that wrinkles have a small effect on force magnitudes. It is thus one purpose of this paper

*Research Student, Department of Engineering, Trumpington Street, Cambridge CB2 1PZ, Student Member AIAA. Email: ab733@cam.ac.uk
†Senior Lecturer, Department of Engineering, Trumpington Street, Cambridge CB2 1PZ, Member AIAA. Email: kas14@cam.ac.uk
‡Lecturer in Aerostructures, Department of Aeronautics, Prince Consort Road, London SW7 2AZ, Member AIAA. Email: m.santer@imperial.ac.uk

to determine whether this assumption is valid. Although much of preceding discussion has been concerned with flat membranes, which are viable for use in telescopes[2] , they can also be curved out-of-plane for more easily focussing the incoming light. This can be achieved by drawing together two membranes separated by a short distance when flat, either by physically attaching them to each other at discrete points in-plane or by generating an electrostatic attractive field between them[3] : in later simulations, an out-of-plane pressure is applied for simplicity. Whatever the origins of the curvature, the performance of the membrane and the effect of its connectivity to the edge structure also have to be assessed in view of their wrinkling behaviour. This is something we begin to explore in this paper.

This paper has three parts. In the first part, we detail an experimental procedure for inducing a variety of wrinkling patterns in nominally flat, polygonal membranes. Small membranes are considered for ease of experimental testing; but they can be compared directly to results from finite element analysis, in order to determine the expected performance of larger membranes. The character of patterns is directly linked to the out-of-plane displacements of membrane, and two photographic techniques are presented that enable these displacements to be recorded generally and to be quantified accurately. We also describe another apparatus in which the membrane is loaded normally by a pressure. This attempt to enable a global membrane curvature is rudimentary, as the membrane is clamped uniformly on its boundary to create a seal so that a vacuum may form on one side. The boundary outline is, however, polygonal, and there is some overlap with the ultimate concept. Furthermore, the experiment can be compared easily to a straightforward computational analysis. Development of a discretely pre-tensioned, pressurised membrane requires more sophistication and will be the subject of further study.

The second part is concerned with finite element analysis of wrinkled membranes. A variety of polygonal membranes are studied in keeping with the enquiry about the influence of the number of sides[1] . With the exception of the triangular[4] and square membranes[5] , such generality is absent from the literature as far as we are aware. We use the commercially-available finite element package, Samcef[6] , to incorporate realistic effects, including a full constitutive material model with plasticity, as well as the precise details of the cable terminations on the membrane vertices. Initially, simulations are compared qualitatively to the previous small-scale laboratory experiments, in order to confirm the wrinkling patterns generated in nominally flat membranes. In doing so, we identify two main types of wrinkles: those with relatively large amplitudes that arise in the bulk of the membrane due to asymmetrical loading, and those with a much finer wrinkling on the free edges when the pre-tensioning is uniform. The sophistication of analysis is also varied by discounting some of the techniques employed and material properties thought to be essential for accuracy but which add computational expense. If the analysis can be simplified without a loss of accuracy, a greater range of membrane geometries can be studied whilst maintaining confidence in the predicted wrinkling formation. In a final set of simulations, we develop predictions of the out-of-plane shape of pre-tensioned, pressurised membranes of the same size proposed before[1] . One aim is to determine the cable forces on the vertices when the tabs connecting each vertex to the cable force are modelled. In our companion paper, they are not included and thus, any potential disparity in the resulting forces for nominally the same practical set-up will be highlighted.

In the third part, we initiate a discussion on the mitigation of wrinkles, principally, by passive means—by exploiting the planform geometry of the membrane, for this is much simpler than using active control in a space-based environment. In particular for flat membranes, the influence of the geometry of the vertex is scrutinised informally, and the effect of "trimming", or scalloping, the free edges to render them gently curved instead of straight is shown to be effective. Finally, we note that the out-of-plane pressure can usefully remove some wrinkles by overwhelming compression in the bulk of membrane.

II. Experiments

(a) Flat membranes

Figure 1 indicates an experimental apparatus for applying discrete loads to the vertices of flat polygonal membranes, in order to seed the formation of wrinkles. The supporting rim is an aluminium ring with 36 equally spaced holes on its circumference through which cables can be threaded for connecting to regular membranes of either 3, 4, 6, 9, 12, 18 or 36 sides.

Initially, the rim was laid flat, and the horizontal cables were directed through the holes to gravitational scale-pans. They were later replaced by self-contained, sprung-loaded devices, as shown. The cable is attached to the end of a threaded rod, which is restrained against an intervening precision spring by means

of a wing-nut and bearing washer: the spring is fixed to the rim. As the wing-nut is tightened, the spring is compressed and the threaded rod is displaced radially, which increases the level of pre-strain (and pre-tension) applied to the membrane. Provided the radial displacement is properly calibrated against the spring force, accurate levels of pre-tension can be applied via displacement control. Figure 1 also shows the tab through which the cable force is delivered to the vertex; following extensive testing, the choice of tab geometry ensured that relatively large forces could be applied to the membrane without causing it to tear, so that substantial wrinkles could be induced. Note also the choice of a hexagonal membrane in the figure: other shapes were made and tested, but the hexagon offered a reasonable diversity of wrinkle patterns without extensive calibration, and is thus the preferred experimental shape.

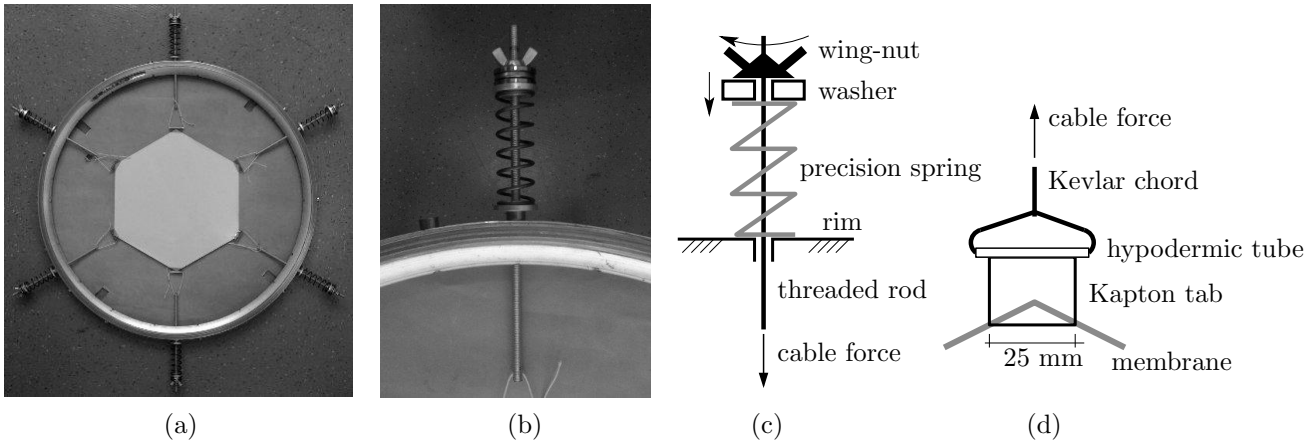

Figure 1. Apparatus for creating wrinkling patterns in a thin hexagonal, Kapton (Young's modulus 2500 MPa, Poisson's ratio 0.34) membrane of diametral width, 300 mm, and thickness, 0.025 mm. Wrinkling follows the application of vertex forces through interconnecting cables. (a) Main apparatus. The circular rim is an aluminium ring with circumferential holes, around which pre-tensioning devices are placed equally, and shown in detail in (b), and schematically in (c): by rotating the uppermost wing-nut, the threaded rod shortens against the precision spring to produce the required cable force. (d) Schematic of the tab detail at each vertex, indicating the distribution of the cable force through a spreading hypodermic tube into a locally thickened tab region of width 25 mm.

Several load cases have been tested in detail. Whilst the reflector concept proposed before[1] is assumed to operate under a nominal biaxial strain state following equal pre-tensions in all cables, it is instructive to consider how the membrane performs when not all of the cables are actively transmitting a pre-tension, as might occur when one or more cables fail. Figure 2 shows four such cases: a biaxial case with equal pre-tensions, two cases with a single plane of loading symmetry for four and two active cables, respectively, and a fourth case with non-uniform cable tensions on either side of the membrane. Beneath each schematic there is a plan-view of the corresponding experiment in which the cable forces are large enough to seed substantial wrinkling patterns, although in the first load case, there are virtually no wrinkles. The particular force values are not of consequence here as we are interested in the qualitative patterns. Note the photographic clarity of patterns, which was achieved as follows.

Each membrane is closely lit by four coloured bulbs—red, green, blue and orange. A photograph is taken, and then again with at least one of the bulbs switched off, and repeatedly so for each bulb being switched off. All photographs are compared, and the one with the best contrast is then selected for demonstrating the particular wrinkling pattern. The process is repeated each time the loading is increased, for example, Fig. 3 details the growth of a major span-wise wrinkle for the third load-case in Fig. 2. But what is also clear from the experiments, and from closer scrutiny of photographs, is the presence of finer, distributed wrinkles close to the free edges: the final sub-figure of Fig. 3 shows an extreme manifestation of such wrinkles when the cable forces are large enough to reveal them. Edge wrinkles are well known from other studies on triangular membranes[4] and are generally observed here in all load cases except for the first biaxial case. Although their presence should not significantly affect the optical performance of the membrane due to their confinement well away from the focussing region, it is important to quantify that they do not persist into the bulk of the membrane: this is explored in more detail in the next section.

The previous photographic technique provides a plan-view but without quantifying the out-of-plane depth

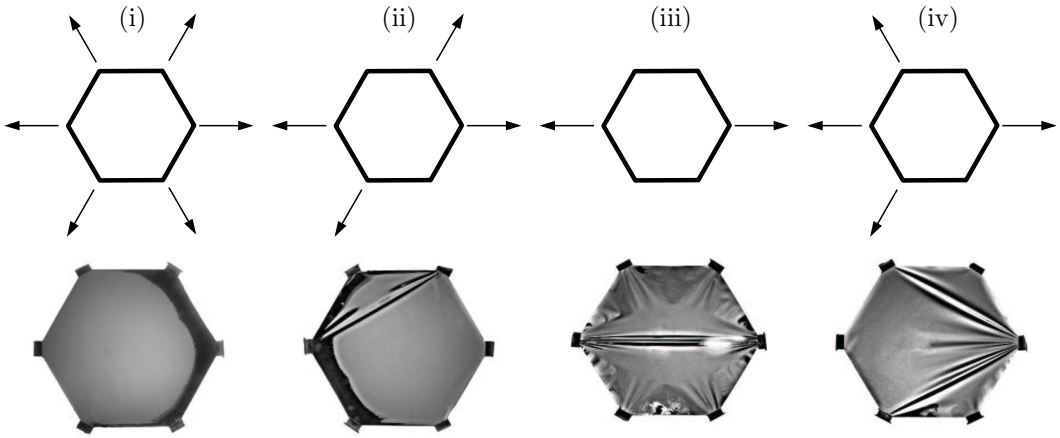

Figure 2. Top row: arrangement of principal cable pre-tensions, indicated by the force vectors, in four typical load cases denoted by (i) to (iv), which feature throughout the rest of this paper. Where no vector is indicated, a very small amount of pre-tension, around 1 N, is applied to the membrane just to overcome the initial slack in the cable. For cases (i) to (iii), the magnitude of the loads applied to each membrane are nominally equal; in case (iv), the net horizontal resultant of the left-side forces is equal to the right-side force. Bottom row: actual wrinkling patterns observed in the membrane from Fig. 1 for each load case directly above when the cable forces are of the order of 50 N. The shadows are deliberately retained in the first two cases, to emphasise edge wrinkles further but which are nonetheless absent from view.

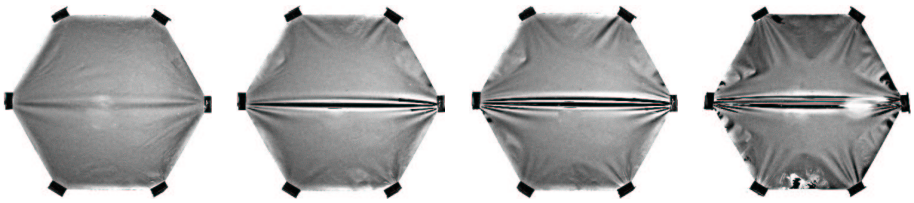

Figure 3. Development of the major wrinkle in load-case (iii) from Fig. 2. From left to right, the cable forces increase from 10 N to 70 N in steps of 20 N. In the final sub-figure, the additional wrinkling spreads from the other vertices as more membrane material is drawn into central wrinkle, resulting in a star-like pattern.

of wrinkles. On the other hand, Fig. 4, shows a digital reconstruction of the membrane distortions for the third load-case after processing via a *photometric stereo*[7] method . A similar lighting arrangement is used but where all bulbs are lit around the membrane. It is sprayed with a thin veneer of white powder to reduce the reflectivity of the surface and a picture is taken using a 10 MP digital camera. Using a bespoke algorithm[7] , the membrane shape is rendered as a set of three-dimensional points in real time, which is converted into a mesh using a software package, *e.g.* Matlab[8] . Artificial lighting is stipulated to create a similar view to the original photograph. The numerical representation of the membrane surface can be used to extract the precise geometry of wrinkling patterns, in order to compare to experimental measurements. This is the subject of on-going study.

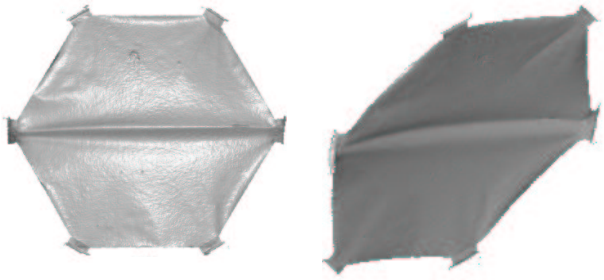

(a) (b)

Figure 4. Load-case (iii) from Fig. 2 subjected to the photometric stereo[7] technique for measuring out-of-plane displacements. (a) Reconstructed plan-view of the membrane with a single span-wise wrinkle. (b) Perspective view which better shows the star-like distortion arising from smaller wrinkles near each corner reported in Fig. 3.

(b) Curved membranes

As noted before, optical membranes are curved for focusing light but must also be pre-tensioned in-plane for a surface smoothness. Our present experiments do not cater for this duality but we are currently developing this capability: Figure 5 shows an intermediate solution, which allows a pressure to be applied to a hexagonal membrane clamped on its entire boundary, thereby enabling out-of-plane curving.

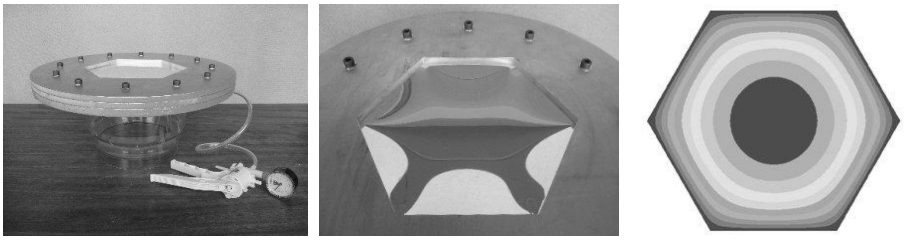

(a.i) (a.ii) (b)

Figure 5. (a) Apparatus for applying a normal pressure to a hexagonal membrane clamped everywhere on its boundary; (a.i) overall detail, which shows the clamping plate sitting on top of a transparent evacuation chamber and connecting pump and pressure gauge: (a.ii) pressurised "inflated" Kapton membrane of diametral width, 240 mm, and thickness 0.025 mm. (b) Plan-view of the out-of-plane displacements of an identical pressurised membrane from a finite element analysis.

The membrane is sealed between two, circular steel plates with a hexagonal cutout of diametral width, 240 mm: this dimension is constrained by the size of the commercial desiccation/evacuation chamber attached and sealed beneath. A Perspex plate with a small hole is attached to the top plate, and permits the pressure on the top-side of the membrane to remain at atmospheric. An adapted micrometer gauge also passes through the hole for measuring the central deflection of membrane as it is drawn downwards during evacuation of the air from inside the chamber. The associated pressure is read via a Bourdon pressure gauge, which was rated to be accurate only for pressures above 10 kPa, and the performance is recorded in Fig. 6 along with predictions from a finite element analysis.

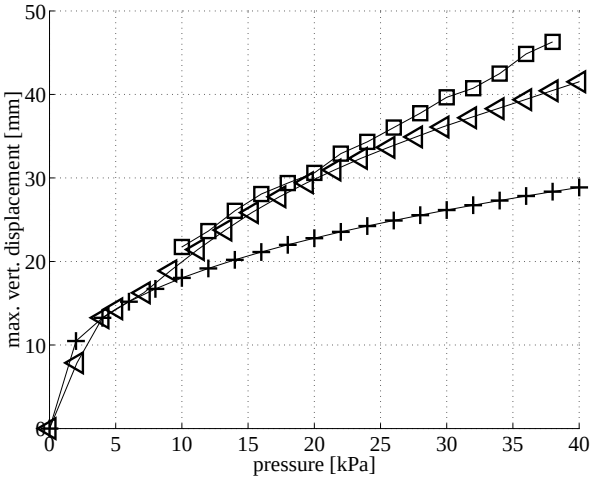

Figure 6. Comparison of central (maximum) displacement of the pressurised Kapton membrane in Fig. 5 between experiment (squares) and finite element analysis with plastic effects (triangles) and without plasticity (crosses): the yield strain of Kapton was measured to be 2.13%. Note that the readings from the pressure gauge were accurate only above 10 kPa, leading to an absence of data in this region.

This is a straightforward, non-linear static analysis using thin shell elements without rotational degrees-of-freedom. The constitutive material model also includes plasticity effects, where the Kapton material is assumed to yield at a measured strain of 2.13%. This inclusion is warranted in the present set-up, as it better captures the experimental trend compared to the "elastic-only" prediction. Indeed, it would appear that the material is yielding at a maximum out-of-plane displacement relative to the membrane size of around $15/240 \approx 6\%$, which is low compared to a specified equivalent of 10% in the proposed full-scale concept. The possibility of the membrane yielding prematurely shape may cause difficulties in controlling the bulk shape for optical propriety, and must be assessed during design. Note, however, that the proposed concept has a much higher ratio of membrane diameter to material thickness compared to the present experiment, which reduces the level of in-plane straining. Also, the discrete boundary support is much more amenable to out-of-plane displacements than the fully built-in case. Furthermore, the analysis performed in the final part of the next section has confirmed that the bulk strains never exceed the yield limit of material in the larger membrane.

III. Finite Element Analysis

(a) Procedure and results

Finite element modelling of the formation of wrinkles in flat membranes is challenging if the membrane is assumed to be perfectly flat, which is most convenient for setting up the initial mesh. The elastic analysis cannot proceed without some out-of-plane distortion, in order to seed the potential for bending and, hence, wrinkling. Therefore, the mesh must be imperfect initially, and one successful approach is to superpose artificial displacements from a stability analysis onto the initially flat membrane before proceeding with main analysis[5] . Here, the flat membrane is pre-tensioned uniformly by loading each vertex up to 1 N, in order to impart some out-of-plane stiffness. The buckled shapes of the first four eigenmodes are then extracted via a linear stability analysis. The corresponding out-of-plane displacements are re-scaled to the same amplitude such that, when these four sets of displacements are added together and then to the flat mesh, the maximum imperfection height is equal to the membrane thickness. Afterwards, the membrane is loaded more significantly at the required vertices in a non-linear analysis following the load cases reported in Fig. 2.

The chosen FEA package is Samcef[6] largely because of the reported success by Samtech—Samcef's developer in collaboration with the European Space Agency on related problems. Each mesh is constructed from up to, approximately, 20000 membrane elements, for which a rotation-free shell hypothesis is specified,

as this is reported to improve convergence during solution[9] , which is performed on a Pentium IV personal computer. The tab detail from Fig. 1(d) is simulated by adding extra triangular layers of material of the same width of tab at each vertex: the cable force is then applied to a vertex node. Although this does not capture exactly the tab detail, the important feature is the local thickening of material around the vertex, as this stiffens the material in bending, which prevents the wrinkles from forming right next to the vertex as seen in practice.

The out-of plane displacements following loading are obtained, showing the number of wrinkles, their amplitudes and their locations on the membrane. The first principal stresses are also distilled, given that wrinkles tend to form in their direction, but a more useful measure of wrinkle location stems from examining the lower, second principal stresses: when they are negative, they indicate compression and hence regions where wrinkles can be expected. Note that, under increasing pre-tension, the wrinkle amplitudes do increase generally but their distribution tends not to once a dominant pattern has formed. Consequently, the compressive "map" is largely invariant in planform after wrinkles have formed, thereby providing useful information without having to specify load magnitudes.

A typical set of results is given in Fig. 7, which ought to be compared with the fourth load-case in Fig. 2. As the pre-tensioning is increased, major wrinkles begin to form by propagating along straight lines between the loaded vertices. These also closely follow the regions of negative principal stresses, which show more clearly thin bands of compression on the free edges where finer wrinkles may be expected in practice. At the end of this simulation, the wrinkling pattern bears a remarkable similarity to the experiment: two major inclined wrinkles are present along with a third central wrinkle spanning halfway across the membrane. Although comparisons to the other load-cases in Fig. 2 are not shown, similar close agreement is observed. One immediate aim of our research is to quantify predictions against data from the previous photometric stereo method, which is the subject of continued work.

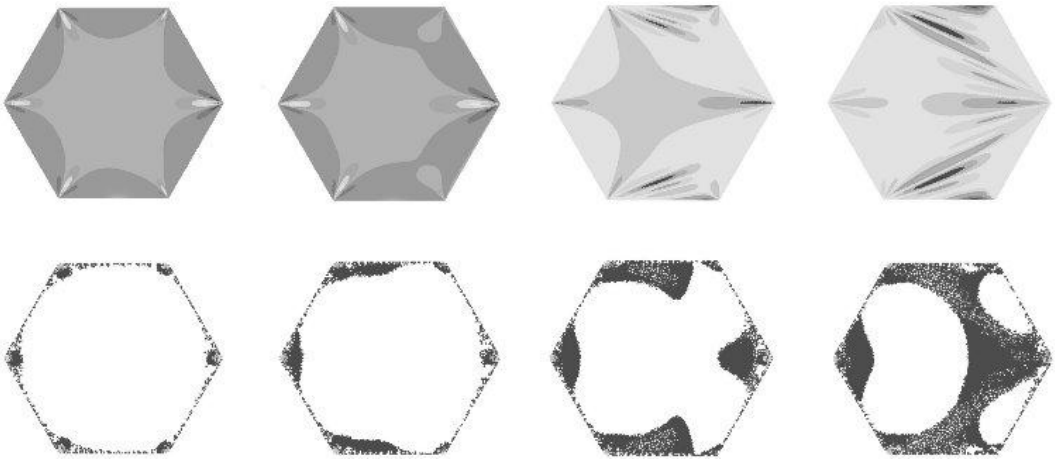

Figure 7. Finite element analysis of load-case (iv) from Fig. 2. The wrinkling pattern occurs evolves under increasing pre-tension from left to right. Top row: variation in the out-of-plane displacements as given by a greater disparity in the contours. Bottom row: regions of compressive principal stress are coloured whilst tensile regions remain as white. Note the correlation between the wrinkled and compressive regions as they evolve for elastic-only behaviour.

In closing, we draw attention to Fig. 8, which compares finite element procedures for the first load-case of a uniformly pre-tensioned membrane. Without seeding an initial imperfection, there is no wrinkling for elastic-only behaviour. This is not unexpected, and when the imperfection is restored, wrinkling is observed. When plasticity is specified in the constitutive material model, wrinkling also occurs, and convergence with elastic-only behaviour is achieved when the corner displacement (pre-tension) is large enough. However, surprisingly, wrinkling occurs for the plastic case when there is *no* initial imperfection. Initially, there is no departure from the elastic-perfectly flat case but it bifurcates suddenly and moves onto the wrinkled path before achieving the same wrinkled state as the others. At present, it is not clear why no imperfection is needed to foster wrinkling in the plastic case but it circumvents the need for a linear stability analysis. We are presently testing this premise on the other load cases.

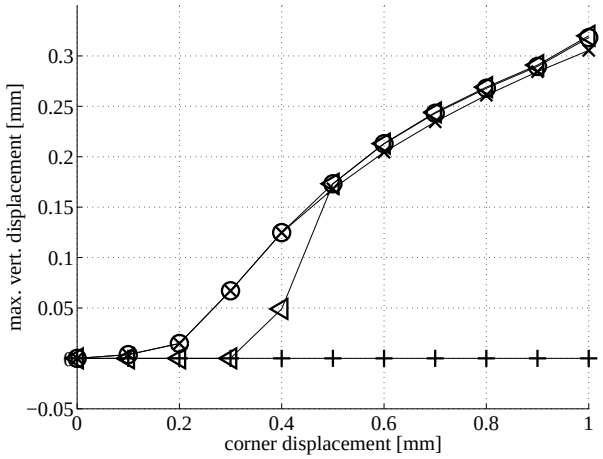

Figure 8. Comparison of finite element procedures for flat membrane wrinkling, for load-case (i). The final pre-tensioning value produces a corner displacement of 1 mm, and the maximum vertical displacement applies to the corresponding wrinkles. The crosses indicate when no initial out-of-plane imperfection is seeded for elastic-only material behaviour; conversely, the "×" curve stems from including imperfections as given by summing equally the first four buckling modes from an eigenvalue analysis. Circles denote analysis with shape imperfections and plasticity effects; triangles relate to a plastic analysis without initial distortions. Note the final convergence between the latter three procedures.

(b) Effect of number of sides

Previously[1] it was concluded that the number of sides, n, of the membrane will not be governed by the structural requirements if $n > 10$. Here, we detail two final sets of simulations where the number of sides of membrane, n, can vary to assess the effect on the wrinkling behaviour. The first set indicates regions of wrinkling in similar-sized membranes with n = 3, 4, 6 and 9, under uniform pre-tension—recall that their distribution is not affected by the pre-tension size once wrinkles have formed, and is shown in Fig. 9.

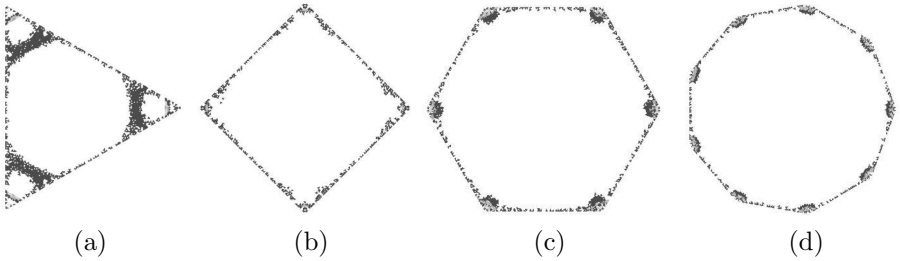

Figure 9. Finite element analysis (elastic) of four Kapton polygon membranes of the same diametral width, 300 mm, and thickness, 0.025 mm, where regions of compressive principal stresses and hence, wrinkles are highlighted. In each case, all cable forces are concentric with the geometric centroid of polygon, thereby inducing a nominal biaxial stress state in the membrane centre. The level of pre-tension is large enough so that the compressive regions are well established: their wrinkles are confined to all vertices and to thin bands along the free edges.

It is certainly clear that wrinkles quickly become confined to the free edges once $n > 3$; only in the triangular case, do they persist radially for some distance beyond the vertex tabs. In the following section, we demonstrate informally a link between the properties of the vertex angle and the formation of radiant wrinkles.

Figure 10 shows the magnitude of the out-of-plane pressure and the resulting cable forces in the full-scale membrane for the indicated geometry, material, levels of pre-tension and maximal out-of-plane displacement. In particular, three sets of results are presented, including theoretical predictions based on an equivalent circular membrane, and finite element analysis with and without the appropriate vertex tab detail, where the

tab is 70 mm wide for this larger membrane. Importantly, the trends are similar but there are clear differences mainly between the computational results, which underpins the importance of properly accounting for the tab detail. It is observed that the pressure and cable forces tend to be higher when vertex tabs are present in the simulation.

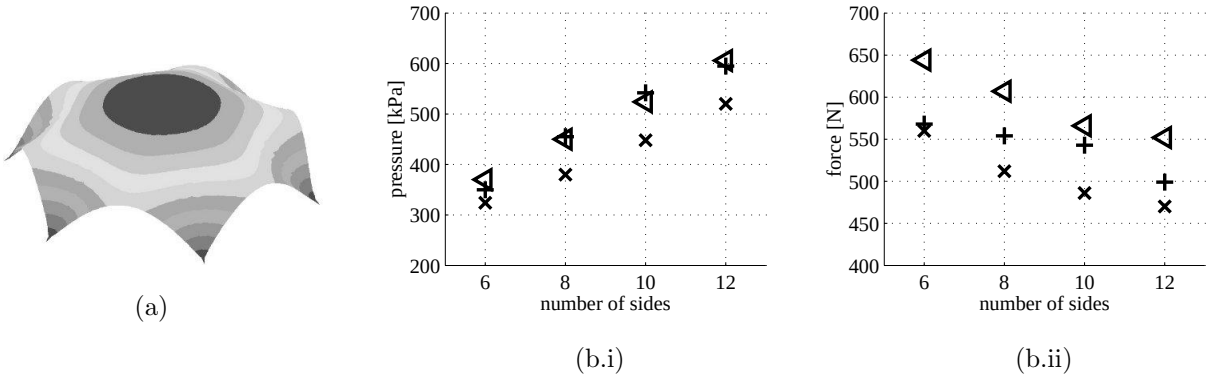

(a) (b.i) (b.ii)

Figure 10. Comparison of pressure and cable force properties for pressurised Mylar (Young's modulus 3790 MPa, Poisson's ratio 0.3) membranes of the indicated number of sides of polygon: the diametral width of each membrane is the same, 2.5 m, as is the thickness, 0.014 mm, as proposed in the full-scale reflector concept[1] . The initial biaxial pre-strain is 15×10^{-6} and is applied uniformly before application of a normal pressure. (a) Out-of-plane deflected shape, amplified threefold for clarity: note that the ratio of maximum displacement to membrane width is 10%. (b) Crosses denote approximate results based on the analytical predictions[1] for a circular membrane; in the same study, "×"'s relate to a wrinkling finite element analysis but without vertex tabs of the type shown in Fig. 1. Triangles apply the present study, which accounts for tabs. (b.i) the pressure needed to generate a central deflection of 250 mm, as specified before[1] ; (b.ii) the corresponding cable forces.

IV. Wrinkle Mitigation

As noted previously, surface anomalies can affect the focussing capabilities of a membrane and thus, mitigating any wrinkles is essential to maintain optical purity. In this section, we show qualitatively how this might be achieved by passive means, by considering first the effect of changes in the membrane geometry for the case in which the membrane is flat, and then by looking at the effect of applied curvature.

Figure 11 highlights the compressive wrinkled regions in two membranes with highly distorted initial shapes, but which are pre-tensioned equally and concentrically on all vertices. Two conclusions become apparent for this nominal biaxial behaviour: that wrinkles tend to form and radiate from acute vertices and not from obtuse ones, and that they persist further into the membrane under an increasing length of adjacent side. The former is reflected in Fig. 9 where only the equilateral triangle has substantial wrinkles in the corners.

Figure 12 shows another mitigating technique[4] where all of the straight sides of the triangular and square membranes are initially scalloped—trimmed—to become gently and uniformly curved in plan. The trimming detail is also indicated, and a large number of wrinkles on the free edges and around the vertices are clearly absent after trimming both membranes, especially so for the triangular one. Finally, Fig. 13 indicates the third load-case from Fig. 2, with a prominent single wrinkle, which is then pressurised without plastic effects to achieve the out-of-plane shape whilst maintaining the vertex displacements required for wrinkling. As can be seen, the wrinkle dissipates as it becomes overwhelmed by the normal deflections due to pressure. There remains, however, sizeable compressive and hence, wrinkled regions at each vertex, which reduce the available membrane area which may be used for focussing.

V. Conclusions

This study has been concerned with the behaviour of polygonal membranes. These are proposed to replace monolithic mirror structures owing to their potential improvement in areal density. The membrane must be

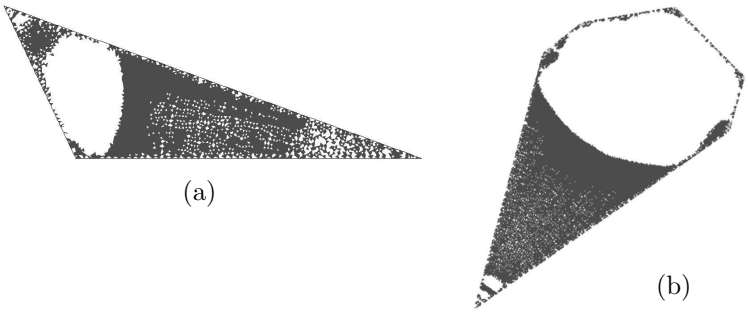

Figure 11. Finite element analysis of pre-tensioned irregular membrane planforms (a) triangular and (b) hexagonal. Only regions of compressive principal stresses are highlighted, which emanate from narrow vertices under biaxial loading.

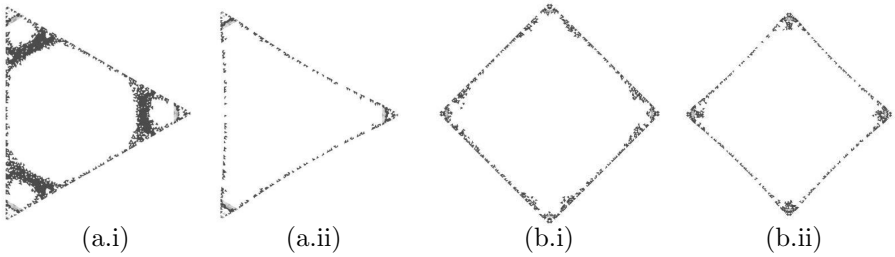

Figure 12. Finite element analysis of the effects of scalloping, or trimming, the free edges to a gentle curvature, in order to mitigate edge wrinkles. (a) Triangular planform with (a.i) straight and (a.ii) trimmed edges, and (b) a square with similar apportions. The overall geometry and material properties are the same as the untrimmed membranes in Fig. 9, and the specified vertex displacements are the same between sub-figures. Trimming results in a uniform circular arc, which indents the straight edge by 2% of its length between tabs.

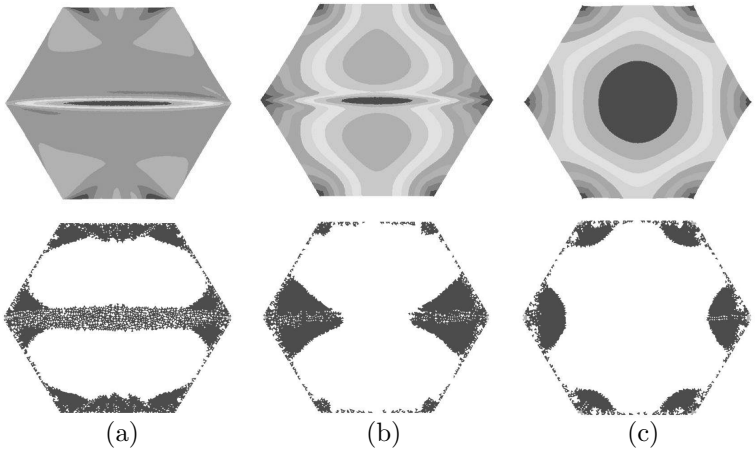

Figure 13. Finite element analysis of load-case (iii) from Fig. 2. (a) The initially flat membrane is pre-tensioned to induce a span-wise wrinkle, where the applied strain is 1.8% at the same vertices. A pressure is then applied to the membrane to cause out-of-plane displacements: (b) intermediate pressure, 4.8 kPa, where the span-wise wrinkle is beginning to dissipate before completely disappearing over the central bulk of the membrane in (c) at 8.0 kPa. Top row: out-of-plane displacements; bottom row: compressive principal stresses.

pre-tensioned initially, in order to impart out-of-plane stiffness for better enabling the correct optical shape during operation. This leads to the possibility of wrinkling since the membrane is very thin: and the problem is exacerbated by the practical arrangement of pre-tensioning through discrete cables, which introduce high, local tensile stresses and, through the Poisson effect, wrinkling-induced compression. The purpose of this study has been to investigate wrinkling in polygonal membranes by means of small-scale experiments and by finite element analysis. The experimental procedure enables us to induce in the membrane a biaxial state of stress as well as to apply asymmetrical loads, as might arise during failure of some of the pre-tensioning cables, and to record the associated wrinkling patterns by novel photographic techniques. With the latter loading, the wrinkling amplitudes are much larger than the membrane thickness whilst uniform pre-tensioning accords much finer wrinkles on the free edges. In both cases, wrinkles also emanate from the cable connections. We have simulated all of these details using finite element analysis and, for each practical load case, we have been able to confirm the generic character of the wrinkling pattern. As part of future work, we aim to compare directly between experiments and simulations.

We have also studied pre-tensioned membranes that are pressurised to produce a curved shape for optical focussing, largely by computational means. The effects of wrinkling and geometrical features, such as the cable connections to the membrane, have been included. This enables the verification of the assumptions made in our companion study[1] for the design of a structural membrane reflector concept. We are currently devising experiments that can allow for both pre-tensioning and pressurisation, in order to better understand the practical membrane performance. Finally, we have discussed methods of mitigating wrinkles, which are the subject of on-going study.

VI. Acknowledgements

A.B. and this work are supported financially by the European Sciences Foundation and by the Engineering and Physical Sciences Research Council, UK, grant number RG48262. The authors thank Prof. Roberto Cipolla, CUED, for his photometric stereo technique, and Prof. Sergio Pellegrino, Caltech, for initiating this project and useful discussions. Finally, we are grateful to Philippe Jetteur of Samtech for his advice on using the finite element software.

References

[1]Santer, M. J., Seffen, K. A., and Bonin, A., "Small-diameter membrane reflector structures," *10th AIAA Gossamer Spacecraft Forum*, 2009.

[2]Stamper, B., Angel, R., Burge, J., and Woolf, N., "Flat membrane mirrors for space telescopes," *Proceedings SPIE, Imaging Technology and Telescopes*, 2000.

[3]Angel, R., Burge, J., Hege, K., Kenworthy, M., and Woolf, N., "Stretched membrane with electrostatic curvature (SMEC): a new technology for ultra-lightweight telescopes," *Proceedings SPIE, UV, Optical and IR Space Telescopes and Instruments*, 2000.

[4]Cunliffe, W., "De-wrinkling of membranes," Tech. Rep. Final year dissertation, Department of Engineering, University of Cambridge, June 2003.

[5]Wong, Y. W. and Pellegrino, S., "Prediction of wrinkle amplitudes in square solar sails: AIAA paper 2003-1982," *44th AIAA/ASME/ASCE/AHS/ASC Structures, Structural Dynamics and Materials Conference*, 2003.

[6]Samcef, *Samcef Version 12.0-03*, Samtech S.A., LIEGE Science Park, Rue des Chasseurs-Ardennais, 8B-4031 Liege (Angleur), Belgium, 2007.

[7]Hernandez, C., Vogiatzis, G., Brostow, G. J., Stenger, B., and Cipolla, R., "Non-Rigid Photometric Stereo with Colored Lights," *Proceedings IEEE, 11th International Conference on Computer Vision*, 2007.

[8]Matlab, *Matlab Version 6.1*, The Mathworks Inc., Natick, MA 01760-2098, United States, 2001.

[9]Samtech, "Project Pastiss, Dossier de Tests, summary report," Tech. rep., LIEGE Science Park, Rue des Chasseurs-Ardennais, 8B-4031 Liege (Angleur), Belgium, 2006.